Response to reviewer comments

We gratefully thank the reviewers for their comments and criticism which we find both well-founded and constructive. Below we answer the comments individually in red and where appropriate also provide our suggested corrections to the manuscript.

On behalf of the authors

Anders T. Pedersen

Reviewer #1

Pedersen and Courtney present a study dealing with a calibration setup for Doppler wind lidars. The setup is a flywheel that is connected to the lidar that is to be calibrated with a solid frame and a tilting mechanism for the lidar. The authors do a great job in deriving the math to obtain a measurement of the flywheel's rotational speed from a sweep of lidar measurements across the wheel's curved surface. They also provide a detailed derivation of the uncertainty components which is best practice. The manuscript is however very vague when it comes to the actual potential of the method for lidar calibration, this is mostly because no targeted accuracy of the calibration is defined to which the results are compared. This makes it difficult to assess the relevance of this work. I recommend major revisions before the manuscript can be accepted for AMT. Below, I give some general comments and more specific comments to parts of the manuscript.

0.1 General comments

• The style of the text is very pessimistic and suggests that the authors do not believe in the value of their work. Why would they want to publish it in this case? I personally believe that there is a lot of value in this work, and I suggest that the authors try to reformulate in a more objective, quantitive way.

We feel that it is our job to be critical about own work and point toward the weak points. However, there should be no doubt that we believe in the value of the work and have therefore reformulated the discussion in a more objective and positive way.

'Nevertheless, the presented measurements and analysis show that the proposed calibration method is not only practically feasible but could actually lead to a significant reduction in calibration uncertainty compared to the current practice. However, there could also be other methods for achieving a similar calibration result. For instance, it seems more straight forward to measure a linear motion along the direction of the beam and this might very well be the case because besides directly measuring the desired parameter, the uncertainties introduced by the angle measurement and assessing the zero-point of the angle scale together with the beam width can be alleviated.'

Also, we have in the introduction tried to clarify the objective of the work and in that way show that the goal is reached, see later comment.

• The mathematical formulations should be revisited. Some of the equations are hard to read. Double subscripts should be omitted, variable names should be consistent and using u for uncertainties in the context of wind measurements is a bit unfortunate. A nomenclature in the appendix would be helpful.

Mathematical expressions have been revisited and corrected; some derivations moved to appendices, see also Specific comments.

The symbol used for uncertainty has been changed to (capital) U.

We prefer keeping the double subscript symbols as we would otherwise need to introduce new variables which would quickly become very confusing.

• The manuscript is a bit hard to read, because the structure is unclear from the beginning, and the goal of the work is not well described in the beginning. Some of the derivations of rather simple geometric relations could be shortened or moved to the appendix to make the manuscript text flow more nicely.

Some less important derivations have been put in appendices and the objective of the manuscript clarified in the introduction.

• My main criticism for the content of the manuscript is, that it does not describe well what are the requirements for calibration accuracy in practice. The authors only briefly mention possible sources of error in Doppler wind lidars, but do not give an idea about the quantity of such errors. How accurate do lidar measurements have to be for the industry or for research purposes? Maybe the calibration accuracy here is good enough after all? In fact, it cannot be known from this experiment if differences between wheel speed estimation through the calibration and reference wheel speed are due to inaccuracy in the calibration setup or the lidar itself.

We have added to the introduction information about current practice for lidar calibrations, uncertainty of these calibrations and the targeted accuracy of the calibration procedure presented in this manuscript to better motivate the work:

'Current practice for calibrating wind lidars is to use cup or sonic anemometers (Courtney, 2013) as reference instrument and the calibration is often limited by the uncertainty of the reference instrument. Even when using sonic anemometers as reference the overall lidar calibration uncertainty is typically of the order of \$1-2\\%\$ (Wagenaar, 2016). This does not do justice to the lidars. We believe that the potential accuracy of wind lidars is much higher than that, lasers are after all very stable instruments and frequency analysis not necessarily faulty, and therefore we propose a new calibration method with a targeted standard uncertainty of \$0.1\\%\$. The result of such an order of magnitude increase in accuracy can hopefully propagate through the wind energy industry as higher accuracy will have significant economic benefits.'

In Sect. 4.1 the uncertainty on the reference speed is estimated to 0.02% which is about a fifth of the total estimated uncertainty, but it is correct that for the overall calibration the lidar uncertainty cannot be distinguished from the rig uncertainty. A calibration will always have an uncertainty and this will be the lowest uncertainty we can ever ascribe to the instrument under test. Therefore we believe that lowering the calibration uncertainty by an order of magnitude can be of importance to the use of wind lidars in the wind industry where people are often looking for gaining a fraction of a percent.

• Until the last sentence of the discussion Section 6 I was wondering if it was not a possibility to measure from zero wind speed perpendicular to the wheel surface to get a more continuous calibration curve. It is a bit unsatisfactory and hard to understand why the tilt angle of the lidar cannot be mechanically adjusted for that.

Yes, it is indeed a bit unsatisfactory. Please see our response to Comment "p.10, l.10f" below.

0.2 Specific comments

• Title: The title is a little bit misleading, because I was expecting to see results of the calibration of the lidar, but actually there are only evaluations about the accuracy of the calibration itself, not the lidar.

Yes, the title could perhaps be more specific although we do not find it directly misleading because what we present is actually a calibration of a wind lidar and the associated uncertainty.

• Introduction:

– p.1,l.20: I think it would be worthwhile to expand on the kind of laser errors that can cause errors of line-of-sight velocity to better motivate the work.

We do not think it is very relevant to list different sources of errors. The point we are trying to make is that without a calibration (comparing against a known reference) we cannot know if the lidar measures correctly. The reason for any inaccuracy is of course very relevant for the lidar manufacturer but for the operator the main concern is if the lidar measures as it should.

– p.2, l.1: Shinder et al. 2013 should be inside the parantheses. The citation style should be checked throughout the manuscript.

All citations have been updated

• Section 2:

– p.2,l.22ff: Since this is a commercial product, I think it would be sufficient to name the manufacturer and give the accuracy of rotation speed measurement. Measurement principle is not so important for this study.

We have shortened the paragraph leaving out technical details about the measuring ring works (P3L5-9)

– Table 1: I recommend to divide the table in two, separating calibration rig properties and lidar properties.

Table has been divided into two as suggested

• Section 3:

– All equations: I suggest to use φ (varphi) to be consistent with the plots.

We have updated the figures such that the same symbol, ϕ, is used as in the text.

– p.4, l.2: Just a suggestion for wording: I do not think it is a severe problem, just a technical one.

Wording changed to:

'… paradox since for the lidar to measure the true tangential wheel speed, and only that, the overlap between laser beam and wheel surface will need to be infinitely small. In this case there will be no backscatter signal to detect! In order to circumvent this paradox it is therefore necessary to measure a different component of the reference speed than the tangential together with the corresponding tilt angle and from that calculate the measured tangential speed.'

– p.4, l.7: Please expand why the resolution of the Doppler spectrum is a problem. It does not define the resolution of the velocity measurement, because the typical MLEs interpolate the spectrum to estimate the Doppler shift. I think the main benefit of several tilt angles / wheel speeds is that the tangential speed can then be extrapolated!?

In the case of a very narrow Doppler spectrum e.g. because the probed speed is extremely uniform the spectral resolution becomes an issue. This case actually occurs in our measurements, when the beam is very narrow and when measuring very close to the wheel top and we therefore think it is worth mentioning. However, we agree that the main benefit is that the speed can be extrapolated.

We have expanded the text:

'Another source of uncertainty, present at any tilt angle, is the speed estimation uncertainty due to the finite resolution of the measured Doppler spectrum which is especially pronounced when using a very narrow laser beam. The narrow beam leads to only a very limited range of projected speeds being sensed confining the Doppler signal to a single spectral bin. However, this uncertainty can be eliminated by scanning over a range of tilt angles or alternatively, a range of wheel speeds.'

– p.4, l.24: I would not call it a trick, it is geometry after all.

'trick' changed to 'approach'

– p.6, l.8f: I think the connection between L'Hospital and the following Taylor's expansion is not made very clear. Maybe Eqs. 9-10 could even be put in the appendix and just be referenced at this point to make it easier to follow the main storyline of the paper.

Agree. Equations 9-10 and accompanying text have been put into Appendix A

– p.7, l.11: Why does part of the beam even have to go above the wheel? Wouldn't it make it easier to just choose tilt angles where the whole beam is on the wheel?

Yes it would, but then we wouldn't know the angle between beam and wheel. The main reason for letting the beam skim above the wheel is to establish as accurately as possible the tilt angle corresponding to a true tangential measurement. We have tried to explain this in Sect. 3.6 and Sect. 3.2.1 where we have reformulated to beginning:

'As mentioned above, Eq. (6) only applies as long as all of the beam is on the wheel but if parts of the beam go above the wheel the relationship between $\frac{V_\text{LOS}}{V_\text{wheel}}$ and θ changes and this is unavoidably what will happen when we try to measure as close as possible to the true tangential speed. It is therefore interesting to take a closer look at the special case characterised by $\phi_0=0$, that is for so small tilt angles that only parts of the beam hit the wheel. Furthermore, measuring in this angular range can be used to estimate the beam width which will be explained in Sect. 3.6:'

– p.9, Eq.17: I think the whole derivation does not have to appear here, especially since the 3D model does not have a significant benefit over the 2D model. It could still be put in the appendix.

Agree. Derivation of Eq. 15 has been put into Appendix B and only the result is left in the main manuscript

– p.10, l.10f: Could the beam width maybe be estimated from the tilt angle sweep if it is done so far until none of the beam hits the wheel any more? Or if instead of trying to hit the tangential, the beam was set to hit the wheel frontal, which would lead to zero velocity measurement?

Yes indeed, and that is what we do and have tried to explain in Sect. 3.6.

Regarding measuring close to perpendicular to the wheel surface, then it is definitely an idea that is worth considering for a future study, but it will require a redesign of the calibration rig (the beam can simply not be tilted enough with the present design) and it has not been possible to perform such a study yet.

– p.12, l.11f: It is not clear to me why the extrapolation from angles larger $\theta 1$ is not the real tangential speed ratio (bi = 1!?).

The finite beam width introduces an offset such that the regime where the speed ratio falls off as -L/R is shifted towards higher tilt angles and an extrapolation from this regime will overestimate the tangential speed. We have tried to illustrate this in Fig. 7 (b) where the dashed line represents the extrapolation.

• Section 4:

– p.14, Eq.27: It would be good to introduce a variable for VLOS Vwheel and use this as subtext in this equation.

Symbol Λ introduced to denote the ratio Vlos/Vwheel.

• Section 5:

– p.16, l.26: "quite well", "some of the truth" and "at least relatively" are such weak statements that I strongly recommend to reformulate.

Wording changed to:

'The first thing to notice is the clear resemblance in the shape of the two curves indicating that this is a valid method for estimating the beam width although the absolute values do not agree. Actually, the values of the calculated widths are about three times higher than the measured, but this is not too disturbing since we are not expecting the measured width to represent the $1/e^2$-width but rather the width from where we can detect a signal.'

– p.20, l.18: %/◦is not a good notation and it is also mixed with %/◦.

Wording changed to: "percent per degree"

– p.23, l.2ff: I was wondering about this possibility throughout the whole derivation of the calibration models for $\theta < \theta 1$. Maybe it should be explained earlier, why it is not possible.

As mentioned above this is more a practical issue that our setup does not allow for such a study and we prefer to keep the short explanation in the discussion. However, we have added a small comment about an implication we see regarding the uncertainty:

'In this case the calibration uncertainty would depend critically on the angle measurement uncertainty'

– p.23, l.25: "its" instead of "it's".

Corected

– p.23, l.19f: Is it enough to calibrate continuous wave lidars at a minimised beam width? What would an industrial calibration have to cover?

We believe that it is sufficient to calibrate at a minimised beam width. Best practice is to use the lowest possible calibration uncertainty which achieved with a minimised beam width and furthermore we see no reason why the actual lidar uncertainty should change with beam width. We have changed 'uncertainty' to 'calibration uncertainty'.

Reviewer #2

General comments

The paper of Pedersen and Courtney is well structured and written. They are thorough in their way of deriving models, uncertainties and finally comparing it to measurements. Their approach to use a flywheel in combination with a Doppler wind lidar seems new and worth publishing (after minor revisions).

Specific comments

Concerning the estimate of $\theta 1$ (P12L5-6 and P16L18-21). Did you also measure backscatter? Why not look at the plot of tilt vs backscatter? I suppose it should be increasing from $\theta 0$ to $\theta 1$ strongly and afterwards only slightly (if at all)? If it turns out that the increase in backscatter shows no point of change around $\theta 1$, just make a different set up where you place something (with a sharp edge) on top of the (not turning) wheel and tilt and measure the backscatter as the beam hits the object first partially and then completely. Now the plot should just show an increase in backscatter from the angle where the beam touches the object partially to the angle where it hits it completely and after that stay constant? The difference could be an estimate for $\Delta\theta$? (To avoid backscatter from walls, use window or something that reflects at an angle as background?). If my thoughts on this are correct but a new setup/measurement is too time consuming please address/discuss this appropriately in the document.

The thoughts are correct and definitely a good idea! Unfortunately, our lidar does not measure the backscatter and we cannot perform the suggested analysis on the available data and reprogramming the lidar and repeating the measurements would be too time consuming. Instead we have added a paragraph to the discussion addressing this issue:

'The uncertainty analysis shows that the main uncertainty contributor is $U_{\Delta\theta}$ which essentially depends on the beam width estimation. An estimate for $\Delta\theta$ based on the tilt angles for the first sporadic and the first stable measurements, respectively, was proposed. Another approach that could potentially reduce this uncertainty is to measure the backscatter level as function of tilt angle. In this way the backscatter signal would increase strongly from θ_0 to θ_1 as the overlap between beam and wheel increases and then remain more or less constant when the entire beam is on the beam. Unfortunately, our lidar in its present state does not measure or store the backscatter level and therefore this approach has not been tested.'

In section 3.1 you describe your approach to rotate around the transceiver lens for the model. But I did not see you describing where the tilt-axis lies relative to the telescope for your measurements. If you raise/lower just the end so it rotates around its lens (As the caption of Fig.2 suggests), please include this information somewhere. If the tilt axis is not going through the lens please also address this (maybe add some text that makes clear that the changes/differences to L and yr are negligible).

The telescope tilts around a point located about 10 cm directly below the lens. This information is added to Sect. 2.

The influence of this is negligible and a comment about this added to Sect. 3.1 :

‘As mentioned in Sect. 2 the physical beam actually rotates around a point situated beneath the lens but for a tilt angle of2.5◦,5which is the maximum attainable in our setup, this leads to a negligible difference for xr and yr of about4 mmand0.1 mm, respectively’

Although it is obvious that no wind speeds are measured because the title says "flywheel calibration"- It is after all a "Doppler wind lidar". As someone who uses a Doppler wind lidar to measure wind speeds it feels a bit weird to read the whole paper and end up just with a calibration "for rotating steel". I of course prefer a lidar that goes through such a quality check, but still... the journal is ATMOSPHERIC Measurement Techniques... Maybe you could add a paragraph about how and why this translates to wind measurements or state that this calibration is meant more as a necessity/possibility than as a sufficiency for Doppler wind lidars quality? (This may be a matter of taste... if you feel all is clear by using the word "calibration" that is also fine)

We have added a paragraph to the introduction addressing this subject:

‘It might seem strange to use a rotating steel wheel as measurement target, after-all the lidar is intended for measuring on small aerosols carried by the wind and not a solid metal target. On the other side, the lidar fundamentally measures a frequency shift in the backscattered light due to a relative motion and it is this frequency shift measurement and the subsequent conversion to a speed we wish to calibrate. The origin of the backscatter is in this connection of less importance. One could, however, envision a scenario where a lidar calibrated in this fashion is used to calibrate another lidar in e.g. a wind tunnel or the free atmosphere. This would lead to a calibration procedure resembling that of the current practice but where the limiting accuracy of a cup anemometer is alleviated.’

Technical corrections

Code and data availability: Pedersen, A. T.: Flywheel calibration of coherent Doppler wind lidar - data, https://doi.org/10.11583/DTU.11991189, 2020.

gives me -> Page not found

Our university library service has been advised about this and data will be available shortly.

https://amt.copernicus.org/preprints/amt-2020-88/ says "Anders Tegtmeier Pedersen and Pedersen Courtney" and the paper itself says "Anders Tegtmeier Pedersen and Michael Courtney"

We will contact AMT about this.

There are a bunch of "r"-index is missing: EQ9, P6L15-16, EQ10, P7L5/6/9/11 In the text and figures, you use different styles of the Greek phi (ϕ/φ). Please make this consistent.

Equations have been corrected and figures updated such that ϕ is used throughout.

You use "best" 5 times in the document. When you say "our best" I get it, but just "best" is a bit bold. Maybe rephrase some occurrences.

Wording changed to ‘our best’

P2L19-20 The reference to Fig.1 makes it seem like we should be able to see the inclinometer on top of the telescope. I don’t see it... maybe use labels / zoom in the Fig.1 or if it is an old picture without inclinometer move the Fig.1 reference to one sentence earlier?

Yes, it is an old photo. Figure reference moved one sentence back.

Added to Fig. 1 caption: ‘Inclinometer not visible in the photo’

P6L8 "this" is ambiguous. Maybe use "the right hand side divided by Vwheel"

Wording changed: ‘…the right hand side divided by…’

EQ8 θ should not be there, right?

No. Removed.

P6L15-16 not listed as equations

Corrected

P8L15 should be yr −R ≤ y ≤ yr + R or−R ≤ y−yr ≤ R, right?

Yes. Manuscript updated.

EQ17 ϕ is missing "r"-index EQ17 I don0t follow the last equal sign. Please explain, expand or correct.

Derivation expanded

P10L4 "as long the" -> "as long as the"

Corrected

P11L14 "cause" -> "causes"

Corrected

P12L10 "arise" -> "arises"

Corrected

P13L8 "wee" -> "we"

Corrected

P14L5 "the are" -> "there are"

Corrected

P14L19 "shown i the" -> "shown in the"

Corrected

P11L18-20 Please check the sentence structure again. The last bit doesn’t seem right. May be "way than"->"way other than". Maybe even rephrase as "direct angle measurement" is ambiguous. Did you mean "direct angle measurement from inclinometer"?

Wording changed to: ‘…other than a direct angle measurement with the inclinometer’

P15L8 "assume" -> "assumed"

Corrected

EQ38 index cc should be bc

Corrected

EQ39 I don0t follow this transformation. Did you swap "wheel" and "LOS"?

Yes. Corrected

P17L3 "0.14m" -> "0.14 mm"

Corrected

P17L7 "Table2" -> "Table 2"

Corrected

P17L15-17 Sentence looks wrong. Maybe "measurement widening" -> "measurement is widening"?

Wording changed to: '…is covered in each measurement which spreads the Doppler signal over several bins'

P19L4 "shape curve" -> "shape the curve"

Corrected

Cosmetic suggestions (These need not be address)

P5L4 "rearranging and inserting into Eq. (1)" with the page break - I found it hard to follow (first time reading), that you also use eq.3 in this step.

Fig.6 An arrow for wRe cos(phir) could be nice, but I guess it overlaps with the redline? (Maybe dashed or dotted arrow?)

Figure updated

P13L1 double usage of "end" is hard to read

Sentence rephraised:

'In the end we therefore arrive at an estimate of the ratio…'

P15L22-26 I would rephrase it... explain/motivate $u\theta w$ differently.

P17L6 "relative uncertainty of" -> "relative uncertainty $u\theta w$ of"

P17L7 "absolute uncertainties can" -> "absolute uncertainties $u\Delta\theta$ can"

Fig.9/10 different colour for residuals lines?

Flywheel calibration of a continuous-wave coherent Doppler wind lidar

Anders Tegtmeier Pedersen[1] and Michael Courtney[1]

[1]Technical University of Denmark – DTU Wind Energy, Frederiksborgvej 399, 4000 Roskilde, Denmark

Correspondence: Anders Tegtmeier Pedersen (antp@dtu.dk)

Abstract. A rig for calibrating a continuous-wave coherent Doppler wind lidar has been constructed. The rig consists of a rotating flywheel on a frame together with an adjustable lidar telescope. The laser beam points toward the rim of the wheel in a plane perpendicular to the wheel's rotation axis, and it can be tilted up and down along the wheel periphery and thereby measure different projections of the tangential speed. The angular speed of the wheel is measured using a high-precision measuring ring fitted to the periphery of the wheel and synchronously logged together with the lidar speed. A simple, geometrical model shows that there is a linear relationship between the measured line-of-sight speed and the beam tilt angle and this is utilised to extrapolate to the tangential speed as measured by the lidar. An analysis of the uncertainties based on the model shows that a standard uncertainty on the measurement of about 0.1% can be achieved, but also that the main source of uncertainty is the width of the laser beam and it's associated uncertainty. Measurements performed with different beam widths confirms this. Other measurements with a minimised beam radius shows that the method in this case performs about equally well for all the tested reference speeds ranging from about $3\ \mathrm{m/s}$ to $18\ \mathrm{m/s}$.

1 Introduction

Wind lidars are often referred to as being 'absolute' instruments by which is meant that, given only the two parameters; the laser wavelength and the frequency at which we sample the backscattered light, we are able to calculate the measured line-of-sight (LOS) speed through the well-known equation $V = \frac{1}{2}\lambda \cdot \Delta f$, ~~Pearson et al. (2002)~~(Pearson et al., 2002). This to some implies that wind lidars are also 'calibration free' since there, in contrast to e.g. cup anemometers, are no empirical constants to be found through a calibration. However, a calibration is fundamentally just a comparison to a reference with a known and traceable uncertainty ~~(Joint Committee for Guides in Metrology (2012))~~(Joint Committee for Guides in Metrology, 2012), and without a calibration we have no way of knowing that the lidar measures correctly; small errors can easily creep into the frequency analysis or the laser wavelength may drift etc. Equally important, by using a reference with known uncertainty traceable to international measurement prototypes, we can assign an uncertainty to the lidar radial speed and claim traceability. The latter is often a requirement in commercial measurements where the outcome can have financial consequences. The uncertainty of the calibration can further be transferred to the test instrument and form the basis for additional operational uncertainty estimates.

~~Therefore, and inspired~~ Current practice for calibrating wind lidars is to use cup or sonic anemometers (Courtney, 2013) as reference instrument and the calibration is often limited by the uncertainty of the reference instrument. Even when using sonic anemometers as reference the overall lidar calibration uncertainty is typically of the order of $1-2\%$ (Wagenaar et al., 2016) . This does not do justice to the lidars. We believe that the potential accuracy of wind lidars is much higher than that, lasers are after all very stable instruments and frequency analysis not necessarily faulty, and therefore we propose a new calibration method with a targeted standard uncertainty of 0.1%. The result of such an order of magnitude increase in accuracy can hopefully propagate through the wind energy industry as higher accuracy will have significant economic benefits.

Inspired by a similar concept commonly used for calibrating Laser Doppler Anemometers (LDAs), ~~Shinder et al. (2013)~~ (Shinder et al., 2013), we have constructed a rig for calibrating Doppler lidars. The rig in essence consists of a frame with a stainless-steel flywheel in one end and an adjustable lidar telescope pointing toward the wheel rim in the other. However, conversely to an LDA system a Doppler lidar measures the velocity component along the laser beam and we therefore use the lidar beam skimming on the circumference rather than impinging the wheel surface perpendicularly as the LDA would do. The telescope is mounted on a pivoting mechanism and with this the laser beam can be tilted and thus different projections of the wheel peripheral speed probed. In addition, we have developed a simple model relating the ratio between the speed sensed by the lidar and the peripheral speed to the beam tilt angle and this method allows us to estimate the true peripheral speed by extrapolation from speeds measured at other angles.

~~This~~ It might seem strange to use a rotating steel wheel as measurement target, after-all the lidar is intended for measuring on small aerosols carried by the wind and not a solid metal target. On the other side, the lidar fundamentally measures a frequency shift in the backscattered light due to a relative motion and it is this frequency shift measurement and the subsequent conversion to a speed we wish to calibrate. The origin of the backscatter is in this connection of less importance. One could, however, envision a scenario where a lidar calibrated in this fashion is used to calibrate another lidar in e.g. a wind tunnel or the free atmosphere. This would lead to a calibration procedure resembling that of the current practice but where the limiting accuracy of a cup anemometer is alleviated.

The manuscript is organised in the following way. First the calibration rig and lidar are described. Then the model describing the relation between the measured line-of-sight speed and tilt angle is gradually developed beginning from a simple ~~2D~~ 1D model to a more realistic 2D model and finally a 3D model. ~~The~~ This model forms the basis of the following suggestion for a calibration procedure and analysis of the various uncertainty contributions. Finally, calibrations performed with different laser beam widths and at different reference speeds are presented.

2 Calibration rig and lidar

The calibration rig consists of an aluminium frame on which is mounted a stainless steel wheel together with the transceiver, or telescope, of the lidar. The wheel has a radius of 286.76 mm with a measured eccentricity of about 0.01 mm and it is coupled

Table 1. Physical properties of the calibration rig~~and lidar~~.

Wheel radius	R	[mm]	286.76
Wheel eccentricity	e	[mm]	0.01
Distance telescope to wheel	L	[m]	1.578
Encoder pulses		[pulse/rev]	1800
Encoder pitch		[μm]	1000±3

directly to a servo motor to control its rotational speed. The telescope is mounted at approximately the same height as the top of the wheel and in such a way that it can be tilted around a horizontal axis parallel to the wheel's rotational axis using a fine threaded adjustment screw~~.~~, see Fig. 1. The pivot point is located approximately 10 cm directly under the lens. On top of the telescope is mounted an inclinometer to measure the tilt angle of the laser beam~~, see Fig. 1.~~.

In order to measure the rotational speed, a high-precision measuring ring is fitted to the periphery of the wheel together with a corresponding measurement head sitting near the bottom of the wheel, ~~AMO GmbH (2013). This measurement system is in essence a transformer with a moving reluctance core; the ring is engraved with reluctance graduations at a pitch of 1000 μm with a precision of ±3 μm which induces voltages~~ (AMO GmbH, 2013). As the wheel rotates the ring induces a voltage in the static measurement head ~~as the wheel rotates~~for each 1000 µm ±3 µm. The output of the system is 1800 TTL pulses per wheel revolution, and the period for six consecutive pulses are measured, and inverted to give the wheel rotational frequency. The physical properties of the calibration rig are summarised in Table 1.

The lidar is a direction sensitive continuous-wave coherent Doppler lidar operated with a 1565 nm fibre laser, ~~Pedersen et al. (2014)~~ (Pedersen et al., 2014). The Doppler spectra are based on a 1024 point discrete Fourier transform (DFT) of the detector output sampled at 120 MHz resulting in a spectrum resolution of 117 kHz or 0.0917 m/s. About 1200 spectra are combined to form one average spectrum at a rate of approximately 100 Hz. Based on the average spectrum the radial speed is estimated as the 50% fractile of the signal exceeding the detection threshold, ~~Angelou et al. (2012)~~(Angelou et al., 2012). Focusing of the laser beam is controlled by adjusting the distance from the laser output fibre to the focusing lens with a micrometer screw. The lens has a 1" diameter and a focal length of 0.10 m. Laser, telescope and detectors are connected by optical fibres. The physical properties of the lidar are summarised in Table 2.

Real-time signals from lidar, inclinometer, and rotation encoder are streamed to a measurement computer which synchronises at 100 Hz and stores the data for post processing.

3 Model and calibration procedure

Using a rotating wheel for calibration has been used with LDAs for many years, ~~Shinder et al. (2013); Bean and Hall (1999); Duncan and K~~ (Shinder et al., 2013; Bean and Hall, 1999; Duncan and Keck, 2009), and as mentioned in Sect. 1 our calibration rig is strongly inspired by what has been done with LDAs. However, unlike LDAs coherent Doppler lidars measure the velocity component

Table 2. Physical properties of the lidar.

Lens diameter	m	0.0254	
Lens focal length	m	0.10	
Laser wavelength	λ	[nm]	1565
Sampling rate detector output	f_s	[MHz]	120
Number of points in DFT	NDFT		1024
Bin width		[m/s]	0.0917
Measurement rate	Hz	100	

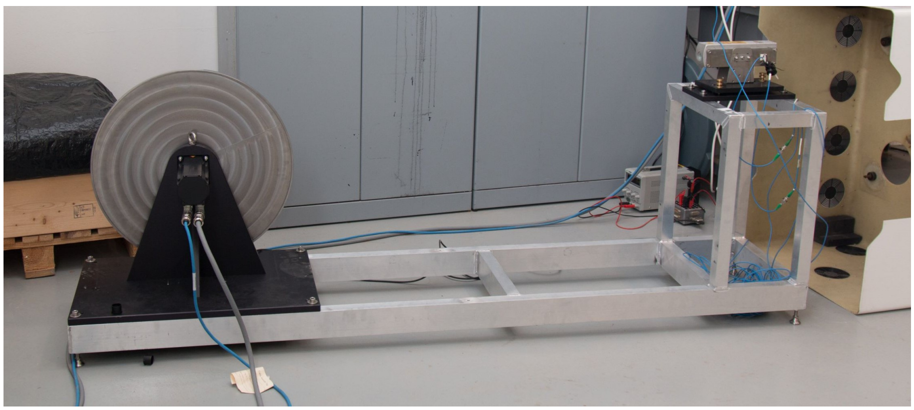

Figure 1. Photo of the calibration rig. To the left is seen the flywheel with cables through which the motor is controlled and to the right the lidar telescope with optical cables connecting it with the laser and detectors. The inclinometer is not visible in the photo.

along the laser beam meaning that the beam must be aligned with and overlapping a tangent of the wheel and this poses a ~~severe problem. For~~ paradox since for the lidar to measure the true tangential wheel speed, and only that, the overlap between laser beam and wheel surface will need to be infinitely small~~and~~. In this case there will be no backscatter signal to detect~~. It~~! In order to circumvent this paradox it is therefore necessary to measure a different component of the reference speed than the tangential together with the corresponding tilt angle and from that calculate the measured tangential speed. Unfortunately, this approach also has some drawbacks in the form of additional uncertainties due to the tilt angle measurement. Another source of uncertainty, present at any tilt angle, is the speed estimation uncertainty due to the finite resolution of the measured Doppler spectrum ~~; this can however~~ which is especially pronounced when using a very narrow laser beam. The narrow beam leads to only a very limited range of projected speeds being sensed confining the Doppler signal to a single spectral bin. However, this uncertainty can be eliminated by scanning over a range of tilt angles or alternatively, a range of wheel speeds. We have developed a model from simple geometric considerations describing the ratio between the tangential wheel speed and the speed

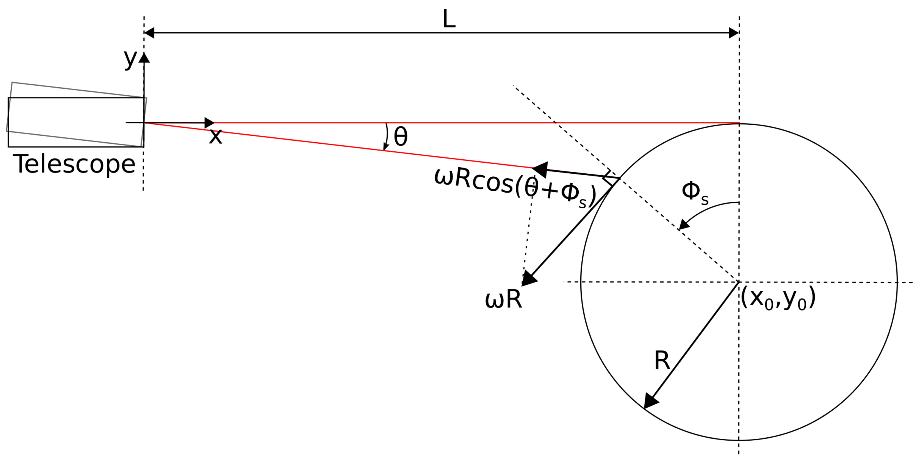

Figure 2. Schematic drawing of the calibration rig illustrating the basic geometry of the rig. The laser beam, illustrated in red, can be tilted using an adjustment screw on the telescope mount.

sensed by the lidar as function of beam tilt angle. The model shows that this relationship is linear and it can therefore be used to make a simple extrapolation back to what would be the tangential wheel speed sensed by the lidar.

In the following subsections the model is derived; first under the approximation that the laser beam has no transverse component (i.e. it is infinitely narrow), during which we establish the relationship between the beam tilt angle, θ, and the skimming angle, ϕ_s, and later for a collimated beam of finite width, w. The model predicts that there are two distinct measurement regimes, one when the entire beam is on the wheel and one when part of the laser beam skims above the wheel, and this has profound influence on interpreting the result. Finally, the suggested procedure for doing the calibration is described.

3.1 Infinitely narrow beam

Figure 2 shows a schematic drawing of the calibration setup. The line-of-sight speed sensed by the lidar (V_LOS) is the wheel's peripheral velocity projected into the direction of the beam at the point of intersection between the wheel surface and laser beam. From Fig. 2 this is seen to be

$$V_\mathrm{LOS} = V_\mathrm{wheel}\cos\left(\phi_\mathrm{s}+\theta\right) = \omega R \cos\left(\phi_\mathrm{s}+\theta\right), \tag{1}$$

where V_wheel is the peripheral speed, ϕ_s is the skimming angle, θ is the beam tilt angle, ω the angular frequency, and R the radius of the wheel.

Now, to find the relation between ϕ_s and θ we can make use of ~~a little trick~~ an approach which will also prove valuable later on; instead of tilting the beam we rotate the centre of the wheel, (x_0, y_0), an angle θ around the centre of the transceiver lens which defines the origo of our coordinate system, see Fig. 3. The new centre of the wheel is denoted (x_r, y_r). From the figure it is clear that the angle, ϕ_r, between the vertical and the intersection point between beam and wheel is

$$\phi_r = \phi_s + \theta, \tag{2}$$

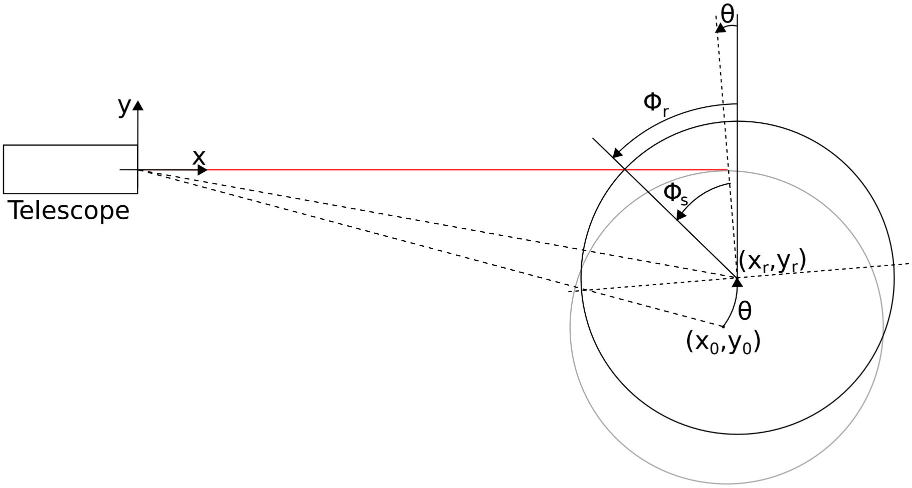

Figure 3. Instead of tilting the beam the centre of the wheel is rotated around the lens centre.

and that

$$\cos(\phi_r) = \frac{-y_r}{R}. \tag{3}$$

From Fig. 2 we see that $(x_0, y_0) = (L, -R)$ and from this we can calculate (x_r, y_r) via the rotation matrix $\underline{\underline{R}}_z(\theta)$

$$\begin{pmatrix} x_r \\ y_r \end{pmatrix} = \underline{\underline{R}}_z(\theta) \begin{pmatrix} x_0 \\ y_0 \end{pmatrix} = \begin{pmatrix} \cos\theta & -\sin\theta \\ \sin\theta & \cos\theta \end{pmatrix} \begin{pmatrix} L \\ -R \end{pmatrix} = \begin{pmatrix} L\cos\theta + R\sin\theta \\ L\sin\theta - R\cos\theta \end{pmatrix}. \tag{4}$$

As mentioned in Sect. 2 the physical beam actually rotates around a point situated beneath the lens but for a tilt angle of 2.5°, which is the maximum attainable in our setup, this leads to a negligible difference for x_r and y_r of about 4 mm and 0.1 mm, respectively. Now, rearranging and inserting into Eq. (1) we finally arrive at

$$\frac{V_{\text{LOS}}}{V_{\text{wheel}}} = \frac{R\cos\theta - L\sin\theta}{R}. \tag{5}$$

~~In our setup θ is small reaching a maximum value of~~ Since the maximum tilt angle is only about 2.5° ~~so~~ we can make the approximations that $\cos\theta = 1$ and $\sin\theta = \theta$ such that

$$\frac{V_{\text{LOS}}}{V_{\text{wheel}}} \approx 1 - \frac{L\theta}{R}. \tag{6}$$

It is thus seen that for small tilt angles there is a linear relationship between ~~$V_{\text{LOS}}/V_{\text{wheel}}$~~ the speed ratio $\frac{V_{\text{LOS}}}{V_{\text{wheel}}}$ and θ and this can be utilised in the calibration procedure.

3.2 Finite width, collimated beam, 2D

Now, a real laser beam is of course not infinitely narrow but has a transverse profile of finite width, e.g. the laser used in this study has a Gaussian profile. We therefore expand the model to include the beam width radius, w, but to begin with limit our selves to the two dimensional case and the assumption that the beam intensity has a constant transverse cross-section, i.e. the intensity profile across the beam has a "top hat shape".

For a beam of finite width a finite part of the wheel perimeter will be illuminated by the laser and thus a range of line-of-sight speeds be measured, see Fig. 4. Each incremental line-of-sight speed will be

$$\mathrm{d}V_{\mathrm{LOS}} = V_{\mathrm{wheel}}\cos\left(\phi_r\right), \tag{7}$$

and these will each contribute a proportion $\mathrm{d}\phi_r/\Delta\phi_r$ of the total speed sensed by the lidar, where ~~$\Delta\phi_r$ $(=\phi_{r_1}-\phi_{r_0})$~~ $\Delta\phi_r = \phi_{r_1}-\phi_{r_0}$ is the total angle subtended by lidar illumination. The total speed contribution V_{LOS} is thus obtained by integrating Eq. (7) whilst normalising by $\Delta\phi_r$

$$V_{\mathrm{LOS}} = \frac{1}{\Delta\phi_r}\int\limits_{\phi_{r_0}}^{\phi_{r_1}} V_{\mathrm{wheel}}\cos\phi+\theta\,\mathrm{d}\phi = \frac{1}{\Delta\phi_r}V_{\mathrm{wheel}}\left(\sin\phi_{r_1}-\sin\phi_{r_0}\right). \tag{8}$$

By applying L'Hospital's rule~~this~~, the right hand side divided by V_{wheel} is easily seen to reduce to $\cos\phi_r$ as ϕ_{r_1} approaches ϕ_{r_0}, i.e. as the beam becomes narrower, and therefore give the same result as in Sect.~~3.1.~~

~~If we apply Taylor's expansion to the third order to Eq. we get~~

$$\begin{aligned}
\frac{V_{\mathrm{LOS}}}{V_{\mathrm{wheel}}} &\equiv \frac{1}{\Delta\phi}\left(\phi_1-\frac{1}{6}\phi_1^3-\phi_0+\frac{1}{6}\phi_0^3\right)\\
&\equiv \frac{1}{\Delta\phi}\left(\Delta\phi-\frac{1}{6}\left(\phi_1^3-\phi_0^3\right)\right)\\
&\equiv 1-\frac{1}{6}(\phi_1^2+\phi_0^2+\phi_1\phi_0),
\end{aligned}$$

~~and if we further make the approximations~~

$$\begin{aligned}
\phi_0 &\equiv \phi_{\mathrm{m}}-\delta,\\
\phi_1 &\equiv \phi_{\mathrm{m}}+\delta,
\end{aligned}$$

~~where $\phi_{r_{\mathrm{m}}}$ is the mean of ϕ_{r_0} and ϕ_{r_1} and δ is a small perturbation we get~~

$$\frac{V_{\mathrm{LOS}}}{V_{\mathrm{wheel}}} = 1-\frac{1}{6}(\phi_1^2+\phi_0^2+\phi_1\phi_0) \equiv 1-\frac{1}{6}\left(3\phi_{\mathrm{m}}^2+\delta^2\right) \approx 1-\frac{1}{2}\phi_{\mathrm{m}}^2 \approx \cos\phi_{r_{\mathrm{m}}},$$

~~which is seen to be equal to Eq.~~ .3.1 and the model is thus mathematically consistent with the 1D model.

~~This means that even~~ Even for a beam of finite width Eq. (6) is a ~~reasonable~~ good approximation to how the ratio $\frac{V_{\mathrm{LOS}}}{V_{\mathrm{Wheel}}}$ changes as the beam is tilted. ~~This can~~ For completeness, a mathematical derivation of this is presented in Appendix. A but from a physical point of view it can intuitively be understood as that the high speed measured at ϕ_1 is more or less balanced by the low speed measured at ϕ_0. However, the approximation only applies as long as the entire beam cross-section is on the wheel; if part of the beam goes above the wheel, as it will for very small tilt angles, the relationship changes as we shall see in Sect. 3.2.1.

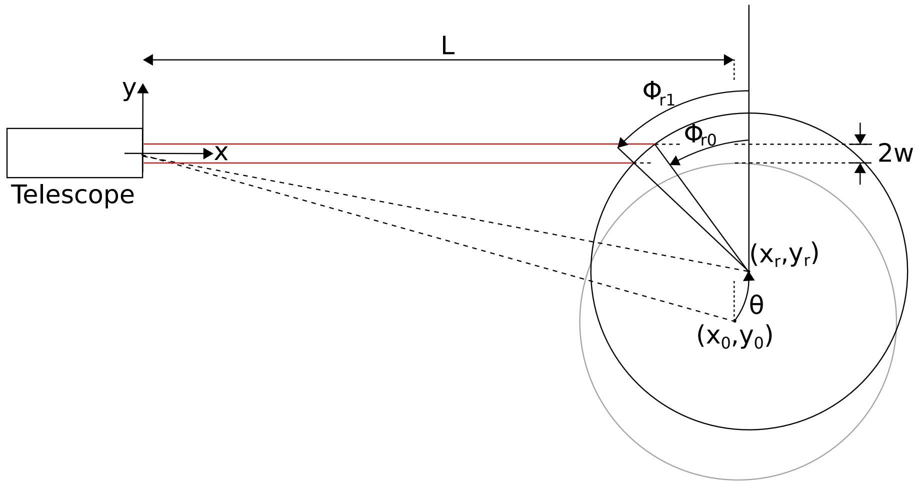

Figure 4. Schematic drawing used to derive the 2D thick beam model. Notice that w is the beam radius and $(x_0, y_0 = L, -R - w)$.

3.2.1 ~~Special case: $\phi_0 = 0$~~Skimming above the wheel

As mentioned above, Eq. (6) only applies as long as all of the beam is on the wheel ~~and it is~~ but if parts of the beam go above the wheel the relationship between $\frac{V_{\mathrm{LOS}}}{V_{\mathrm{wheel}}}$ and θ changes and this is unavoidably what will happen when we try to measure as close as possible to the true tangential speed. It is therefore interesting to take a closer look at the special case ~~when~~ characterised by $\phi_0 = 0$, that is for so small tilt angles that only parts of the beam ~~go above~~ hit the wheel. ~~In that case~~ Furthermore, measuring in this angular range can be used to estimate the beam width which will be explained in Sect. 3.6:

When skimming above the wheel Eq. (8) reduces to

$$\frac{V_{\mathrm{LOS}}}{V_{\mathrm{wheel}}} = \frac{1}{\phi_{r_1}} \left(\sin(\phi_{r_1}) \right), \tag{9}$$

and if we Taylor expand we get

$$\frac{V_{\mathrm{LOS}}}{V_{\mathrm{wheel}}} = 1 - \frac{1}{6} \phi_{r_1}^2 . \tag{10}$$

This means that as long as only a part of the beam is impinging on the wheel the sensitivity to the tilt angle is only a third compared to when the entire beam illuminates the wheel. The range of angles to which this applies obviously depends on the beam width. The angle where the top of the beam first touches the wheel, i.e. when the entire beam is on the wheel, is denoted θ_1 and is calculated through

$$\theta_1 = \arctan\left(\frac{2w}{L} \right) . \tag{11}$$

3.3 3D model

In the previous section we modelled the laser beam intensity profile as a 2D top-hat shape. This is in conflict with the physical reality in two ways; firstly, confining the model to two dimensions effectively means that we are assuming the beam cross-section to be square and not round and secondly the real laser beam has a Gaussian intensity profile and not a top-hap shape. To take these facts into account we must therefore expand the model to three dimensions.

Still assuming that the beam is collimated we can model the beam as a cylinder of radius w centred around the x-axis

$$y^2 + z^2 = w^2, \tag{12}$$

and the wheel as a cylinder along the z-axis and centred around (x_r, y_r)

$$(x - x_r)^2 + (y - y_r)^2 = R^2. \tag{13}$$

The x-coordinates of the overlap between beam and wheel in the rotated frame of reference is found by solving Eq. (13)

$$x = -\sqrt{R^2 - (y - y_r)^2} + x_r, \tag{14}$$

where $\cancel{y \leq R + y_r}$ $y_r - R \leq y \leq y_r + R$ and the sign of the square root is chosen such that only parts of the wheel facing the telescope are illuminated. The corresponding y and z-coordinates are governed by Eq. (12) such that $(y_r, z_r) = (y, z)$. It should be noticed that in this way the overlap between wheel and beam has been parametrisised into a function of y and z i.e. $g(x, y, z) = g(X(y), y, z)$.

In order to find the ratio $\frac{V_{\text{LOS}}}{V_{\text{Wheel}}}$ we follow the same procedure as outlined in Sect. 3.2 by integrating all the speed contributions and normalise by the area of the illuminated surface, $\mathcal{S}$. This can be done by calculating the surface integrals

$$\frac{V_{\text{LOS}}}{V_{\text{Ref}}} = \frac{\iint_{\mathcal{S}} I(y,z)\cos\phi \,\mathrm{d}S}{Ar(\mathcal{S})} \frac{\iint_{\mathcal{S}} I(y,z)\cos\phi_r \,\mathrm{d}S}{Ar(\mathcal{S})}$$

$$= \frac{\iint I(y,z)\cos\phi \sqrt{1 + \left(\frac{\partial X(y)}{\partial y}\right)^2 + \left(\frac{\partial X(y)}{\partial z}\right)^2}\,\mathrm{d}y\mathrm{d}z}{\iint \sqrt{1 + \left(\frac{\partial X(y)}{\partial y}\right)^2 + \left(\frac{\partial X(y)}{\partial z}\right)^2}\,\mathrm{d}y\mathrm{d}z} = \frac{\iint I(y,z)\frac{y - y_r}{R} \sqrt{1 + \left(\frac{\partial X(y)}{\partial y}\right)^2 + \left(\frac{\partial X(y)}{\partial z}\right)^2}\,\mathrm{d}y\mathrm{d}z}{\iint \sqrt{1 + \left(\frac{\partial X(y)}{\partial y}\right)^2 + \left(\frac{\partial X(y)}{\partial z}\right)^2}\,\mathrm{d}y\mathrm{d}z} = \frac{\iint I(y,z)\frac{y - y_r}{R} \sqrt{1 \cdots}}{\iint \sqrt{1 + \left(\cdots\right.}}$$

where $I(y, z)$ is the beam intensity profile. The full derivation of Eq. (15) can be found in Appendix B.

3.4 Model comparison

3.5 ~~Model comparison~~

In order to compare the different models from the simple narrow beam approximation and 2D top hat beam to the full 3D Gaussian beam a numerical evaluation of each has been performed for a beam radius of 2.5 mm ($1/e^2$-radius for the Gaussian ~~profiles~~profile) and plotted together as function of tilt angle in Fig. 5. The left plot shows the models evaluated from $\theta = 0 - 1^\circ$ and the right is a close-up focusing on the transition range where more and more of the beam falls on the wheel. The values used for R and L are the same as for the actual calibration rig.

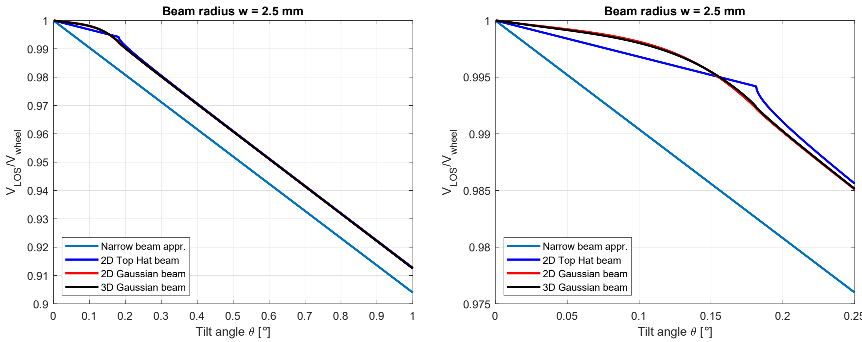

Figure 5. Comparison of the different models evaluated for tilt angles from $0-1^\circ$ to the left and to the right a close-up focusing on the shallow angles where only a part of the beam touches the wheel. For the chosen beam radius $\theta_1 = 0.18^\circ$.

Starting from angles larger than θ_1 we see that all the models fall off with the same slope as predicted by the narrow beam approximation. Again, this indicates that as long as the entire beam is on the wheel the sensitivity to a change in tilt angle is the same for all beam widths and we can use Eq. (6) to calculate this sensitivity. On the other hand it is also clear that the beam width introduces an offset between the narrow beam and finite width models such that the wider beam measures a slightly higher speed than the narrow. This can be seen as the upper and lower parts of the beam not balancing each other perfectly; because of the curvature of the wheel the upper part spreads over a wider part of the wheel and therefore a wider range of speeds. This means that the absolute lidar measurement for a given tilt angle depends on the beam width, and it is therefore critical to know this.

For angles smaller than θ_1 the models stand out more clearly from each other. The 2D beam with a top hat transverse profile drops linearly from $\theta = 0^\circ$ to θ_1 where there is an abrupt change followed by a non-linear change in slope but soon it tends toward slope of the narrow beam. This abrupt change is due the discontinuous nature of the assumed beam profile. It should be noted though that due to the abrupt change the Taylor expansions in Eqs. (6) and (10) do actually not meet in θ_1. The two beams with a Gaussian profile behave differently with a smooth transition from the two regimes because near the edges of the beam the laser intensity is lower and therefore contributes less to the individual measurement. It is interesting to see how similar the two Gaussian models behave indicating that including the third dimension is not critical as long as a Gaussian transverse profile is used.

3.5 Wheel eccentricity

As written in Sect. 2 the wheel when mounted on the servo motor has an eccentricity of about 0.01 mm. This eccentricity may come from either the wheel itself or from the mounting on the motor so that the wheel centre and centre of rotation is not perfectly aligned. In order to model the eccentricity and its effect on the calibration we will here assume the latter meaning that we model the wheel as being ideal but with it's centre off-sat from the centre of rotation by the amount e. Furthermore, we limit ourselves to regard the beam as having no transverse extent as we did in Sect. 3.1.

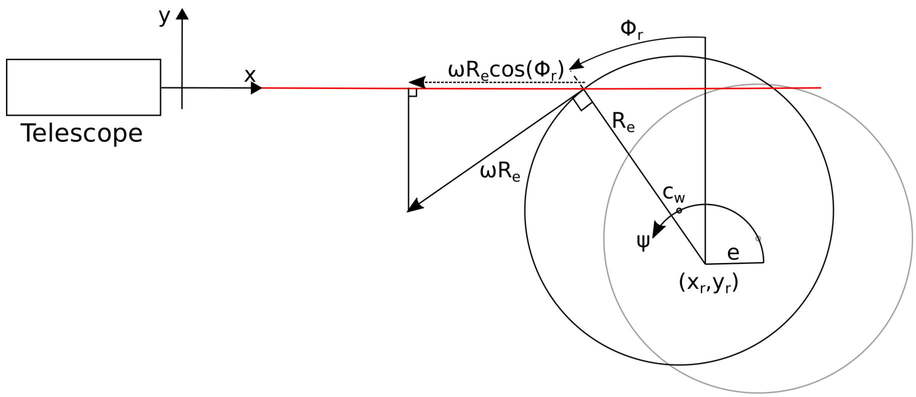

Figure 6. Schematic drawing of the influence of the wheel not rotating around its centre point. The wheel rotates around the point (x_r, y_r) which is off-sat from the wheel centre, c_w, by e.

Figure 6 shows a schematic drawing of the situation adopting the method of rotating the centre of rotation around the lens. The wheel rotates around the point (x_r, y_r) and the centre of the wheel, c_w, therefore follows a circle of radius e around it. The tangential speed at the intersection between wheel and beam is proportional to the distance, R_e, from the rotation centre to the intersection point and the proportionality constant is of course the angular velocity, ω. R_e is a function of the rotation angle ψ. The lidar measures the projection of the tangential speed onto the laser beam and is thus given by $V_\mathrm{LOS} = \omega R_e(\psi)\cos\phi_r$. From the drawing we can see that that

$$\cos\phi_r = \frac{-y_r}{R_e(\psi)} \Rightarrow V_\mathrm{LOS} = \omega R_e(\psi)\frac{-y_r}{R_e(\psi)} = -\omega y_r. \quad (16)$$

This means that the dependence on ψ disappears and the measured line-of-sight speed will be the same for all rotation angles. Now, as the wheel rotates it can happen that the intersection lies to the right of the point x_r, as exemplified by the gray-shaded circle, such that ϕ_r becomes negative, but because cosine is an even function the measured speed will still be the same. However, it is important to note that the measurement is not unaffected by the eccentricity because the radius of the wheel effectively becomes $R+e$ and is therefore larger than in the non-eccentric case. Also for very small tilt angles there will be a part of the wheel not being illuminated during a rotation and no measurement made. Another thing to notice is that this conclusion will not hold for the thick beam, but as we have seen the narrow beam is really a very good approximation to the general case for angles larger than θ_1 which are the angles of interest for the calibration.

3.6 Calibration procedure

As we have seen above our model predicts that there is a linear relationship between the ratio $\frac{V_\mathrm{LOS}}{V_\mathrm{wheel}}$ and the tilt angle θ. This means that we can in principle measure the projected speed at any tilt angle larger than θ_1 and extrapolate back to the speed at θ_0 ($\theta = 0$), i.e. where the bottom of the beam first touches the wheel, via Eq. (6). However, instead of a single measurement we choose to measure the projected speed over a range of tilt angles and fit a straight line to the measured values and in that way do the extrapolation based on a number of measurements. This is in practice done by slowly turning the tilt adjustment screw

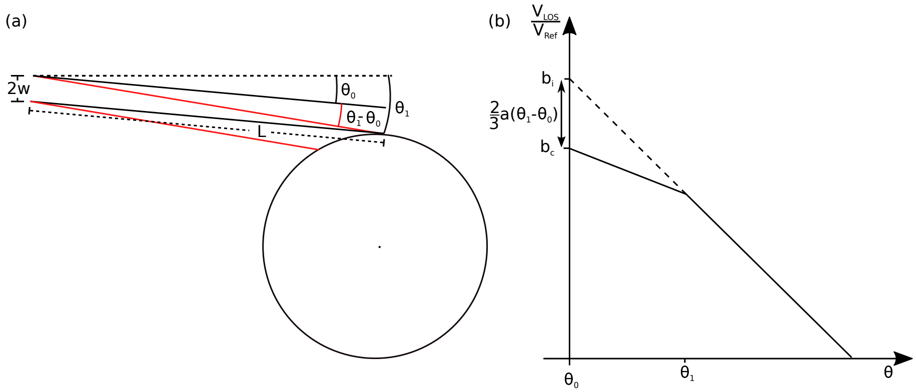

Figure 7. (a) Illustration of the definition of θ_0 and θ_1. θ_0 is the angle compared to horizontal where the bottom of the beam first touches the wheel (beam drawn in black) and correspondingly θ_1 is the angle where top of the beam first touches the wheel (red beam). (b) Illustration of the relation between the angles θ_0 and θ_1, and the fit intercept b_i and the corrected intercept b_c.

on the telescope while synchronously logging V_{wheel}, V_{LOS} and θ. This method furthermore has the advantage of not relying on a single lidar measurement which can be prone to discretisation uncertainty on the speed estimation. The change in angle ~~cause~~ causes changes in the LOS speed that span several frequency bin widths and fitting over this range of angles will tend to average out the errors on the individual measurements.

The difficulty with the method lies in establishing the angles θ_0 and θ_1 i.e. where the beam just starts to touch the wheel and when the entire beam is on the wheel, as illustrated in Fig. 7(a). In our setup the telescope is not perfectly aligned horizontally with the top of the wheel and therefore the laser beam is not perfectly horizontal at θ_0 as shown ~~i~~ in the figure and it is therefore necessary to establish θ_0 in a different way ~~than from~~ other than a direct angle measurement with the inclinometer. For extremely shallow tilts the lidar only occasionally detects a signal, maybe due the slight eccentricity of the wheel or differences in the surface characteristic meaning that some parts of the wheel perimeter extends farther into the laser beam or reflects stronger than others. We choose the angle of this first sporadic signal as our best estimate for θ_0.

The second angle, θ_1, is more difficult to find and is more important for the overall calibration uncertainty. As the beam is slowly lowered from θ_0 the gaps between meaningful measurements become shorter and fewer until eventually a continuous lidar signal is achieved. This means that enough of the beam is now touching the wheel for a signal to be detected for all rotation angles and we choose the angle where this first occurs as the our best estimate for θ_1. Effectively we have thereby also estimated the beam radius as

$$w_{\mathrm{est}} = \frac{L \cdot \tan \Delta\theta}{2}, \tag{17}$$

where $\Delta\theta = \theta_1 - \theta_0$.

Another complication to the calibration ~~arise~~ arises due to the offset introduced by the finite beam width as explained in Sect. 3.4 and illustrated in Fig. 7(b). From the figure it is obvious that extrapolating from angles larger than θ_1 will lead to an overestimation of the speed at θ_0 and it is therefore necessary to compensate for this. We will do this via Eqs. (6) and (10) which states that the speed ratio is

$$\frac{V_{\text{LOS}}}{V_{\text{Wheel}}} = \begin{cases} 1 - \frac{1}{3}a\theta, & \text{for } \theta \leq \theta_1 \\ 1 - a\theta, & \text{for } \theta \geq \theta_1, \end{cases} \tag{18}$$

where $a = \frac{-L}{R}$ is the slope predicted by the models but instead we will use the slope of the actual linear regression while assuming that the $\frac{1}{3}$ relationship still holds. From this the overestimation can be found to be

$$\text{OE} = \frac{2}{3}a(\theta_1 - \theta_0). \tag{19}$$

In the end we therefore ~~end up with~~ arrive at an estimate of the ratio between speed measured by the lidar and the reference wheel speed given as

$$\left(\frac{V_{\text{LOS}}}{V_{\text{Wheel}}}\right)_{\text{est}} = b_i - \text{OE} = b_c, \tag{20}$$

where b_i is the intercept of the fitted straight line at θ_0 and b_c is the compensated intercept. As we saw in Sect. 3.4, Eq. (18) is strictly not correct because of the non-linear drop in $\frac{V_{\text{LOS}}}{V_{\text{Ref}}}$ close to θ_1 as shown in Fig. 5, but for small values of w the resulting error is small.

4 Uncertainties

In this section ~~wee~~ we will give an estimate of the uncertainties associated with the various parameters going into the calibration and of course the overall calibration uncertainty. First the uncertainty on the reference speed is estimated, then the uncertainty on the tangential speed measured by the lidar and finally we combine it into a total calibration uncertainty.

4.1 Uncertainty of reference speed (wheel)

From Eq. (1) we know that the speed of the wheel is given as

$$V_{\text{wheel}} = \omega R, \tag{21}$$

and the uncertainty, U, on this can be obtained by applying the GUM model, ~~Joint Committee for Guides in Metrology (2008)~~ (Joint Committee for Guides in Metrology, 2008) and assuming that the uncertainties on the radius and on the rotational speed are uncorrelated

$$uU^2_{V_{\text{wheel}}} = \left(uU_R \frac{\partial V_{\text{wheel}}}{\partial R}\right)^2 + \left(uU_\omega \frac{\partial V_{\text{wheel}}}{\partial \omega}\right)^2 = uU^2_{\text{R}}\omega^2 + uU^2_\omega R^2, \tag{22}$$

which in relative terms becomes

$$\frac{u^2_{V_{\text{wheel}}}}{V^2_{\text{wheel}}}\frac{U^2_{V_{\text{wheel}}}}{V^2_{\text{wheel}}} = \frac{u^2_R}{R^2}\frac{U^2_R}{R^2} + \frac{u^2_\omega}{\omega^2}\frac{U^2_\omega}{\omega^2}. \tag{23}$$

To get an estimate of the relative uncertainty we will assume an accuracy of 0.05 mm for the wheel radius and that the rotational frequency measurement is derived from a reference frequency that itself has an accuracy of 10^{-5} (10 ppm). Inserting into Eq. (23) gives

$$\cancel{\frac{u^2_{V_{\text{wheel}}}}{V^2_{\text{wheel}}}}\frac{U^2_{V_{\text{wheel}}}}{V^2_{\text{wheel}}} = \left(\frac{0.05\text{ mm}}{286.76\text{ mm}}\right)^2 + \left(10^{-5}\right)^2 = \left(1.75\cdot 10^{-4}\right)^2. \tag{24}$$

The standard uncertainty of the wheel speed is thus of the order of 0.02%.

The calibration flywheel is made of stainless steel which has a thermal expansion of the order $16\cdot 10^{-6}$ /K, ~~Cverna (2002)~~ (Cverna, 2002). Thus a change in temperature between the room where the radius was measured and the calibration room of 1 K will lead to a change in the reference speed of the same proportion. The temperature has not been monitored during these measurements but assigning an uncertainty of 3 K will lead to a relative uncertainty of 0.0048% and therefore not contribute significantly to the overall uncertainty.

4.2 Uncertainty of V_{wheel} measured by the lidar

With the calibration procedure suggested here the laser beam is slowly tilted more and more covering a wide range of projected speeds. Since the response in V_{LOS} to a change in θ is almost linear it is possible to extrapolate back to the angle θ_0 by fitting a straight line to the measured data. However, this indirect way of determining the tangential wheel speed is of course associated with different uncertainty contributions. Firstly ~~the~~ there are the tilt angles, both the direct angle measurement but also very importantly the estimation of θ_0 and θ_1. Secondly there are uncertainties associated with the fit where noise in the measured values will lead to uncertainties in the forecasted slope and intercept.

Let us begin by looking at the uncertainty of the non-compensated intercept b_i. This is obtained from a linear regression which has an inherent uncertainty depending on the number of points in the regression and the level of noise in the measurements. The standard error of the regression, SE, can be calculated as

$$SE = \sqrt{\frac{n-1}{n-2}}\left(\sigma_{\cancel{\frac{V_{\text{LOS}}}{V_{\text{wheel}}}}\Lambda}^{2} - a^2\sigma_\theta^2\right), \tag{25}$$

where where we have introduced symbol $\Lambda = \frac{V_{\text{LOS}}}{V_{\text{wheel}}}$, n is the number of observations and σ is the standard deviation, ~~Lee and Seber (2003)~~ (Lee and Seber, 2003). SE can be regarded as the standard deviation of the noise in the data and can be used to calculate the standard error of the estimated slope, SE_a and intercept, SE_b

$$SE_a = \frac{SE}{\sqrt{n}\sigma_\theta}, \tag{26}$$

$$SE_b = \frac{SE}{\sqrt{n}}\cdot\sqrt{1+\frac{\langle\theta\rangle^2}{\sigma_\theta^2}}, \tag{27}$$

where $\langle\theta\rangle$ is the average of the measured tilt angles. As can be seen SE_a and SE_b depend inversely on the square root of number of observations and for the actual calibrations in this study the relative SE_a is of the order $1\cdot 10^{-4}$ or 0.01% and SE_b

about a tenth of that which is so small in comparison to other contributions that they can be disregarded. Another contribution to the b_i uncertainty is the estimation of θ_0. Since the intercept between the extrapolation and the ordinate is taken to be the tangential wheel speed measured by the lidar it is clear that the position of θ_0 and the uncertainty of this is of great importance for the measured speed and it's uncertainty. As mentioned in Sect. 3.6, θ_0 is defined as the angle where the lidar first starts to pick up sporadic backscatter signals from the wheel surface but there is still an uncertainty associated with this due to the finite resolution, $\delta\theta$, of the inclinometer used to measure tilt angles. Assuming that the true θ_0 is equally likely anywhere within the resolution range (a rectangular probability distribution), the uncertainty on θ_0 can be found as

$$uU_{\theta_0} = \frac{\delta\theta}{2\sqrt{3}}. \tag{28}$$

The squared uncertainty on the intercept due to θ_0 is thus

$$uU_{b_i}^2 = \left(\frac{\delta\theta}{2\sqrt{3}} \cdot a\right)^2, \tag{29}$$

where a is the slope of the extrapolation.The resolution of the tilt measurement is $\delta\theta = 0.01°$ leading to a standard uncertainty of ~~$u_{b_i} = 0.028\%$~~ $U_{b_i} = 0.028\%$ when applying a slope of ~~$9.5\%/°$~~ 9.5 percent per degree as is found in the measurements, see Sect. 5.1. This uncertainty is of the same order as that of the wheel speed.

We know that b_i leads to an overestimation of the speed measured by the lidar and that we need to compensate for this. From Eq. (20) we know that the calibration value compensated for the beam width is given as

$$b_c = b_i - \frac{2}{3}a\Delta\theta, \tag{30}$$

and the uncertainty on this can thus be estimated through

$$\begin{aligned} uU_{b_c}^2 &= uU_{b_i}^2\left(\frac{\partial b_c}{\partial b_i}\right)^2 + uU_a^2\left(\frac{\partial b_c}{\partial a}\right)^2 + uU_{\Delta\theta}^2\left(\frac{\partial b_c}{\partial \Delta\theta}\right)^2 \\ &= uU_{b_i}^2 + uU_a^2\left(-\frac{2}{3}\Delta\theta\right)^2 + uU_{\Delta\theta}^2\left(-\frac{2}{3}a\right)^2, \end{aligned} \tag{31}$$

where we have assumed that the uncertainties of the input parameters are uncorrelated. ~~u_{b_i} and u_a~~ U_{b_i} and U_a have both been estimated above and in the following we will find an estimate for ~~$u_{\Delta\theta}$~~ $U_{\Delta\theta}$.

We will assume that the measurement of θ_0 and θ_1 are each associated with two uncertainty contributions ~~u_{θ_M} and $u_{\theta,D}$. $u_{\theta,M}$~~ $U_{\theta M}$ and $U_{\theta D}$. $U_{\theta M}$ is related to the absolute measurement of θ_0 or θ_1 and could e.g. be due to a gain or offset error, and ~~u_{θ_D}~~ $U_{\theta D}$ is a discrimination uncertainty due to the finite resolution of the inclinometer. ~~θ_{0M} and θ_{1M}~~ $U_{\theta_0 M}$ and $U_{\theta_1 M}$ are correlated because ~~they~~ the angles are measured using the same gauge whereas ~~θ_{0D} and θ_{1D}~~ $U_{\theta_0 D}$ and $U_{\theta_1 D}$ are uncorrelated. We can therefore find the squared uncertainty on $\Delta\theta = \theta_1 - \theta_0$ as

$$\begin{aligned} uU_{\Delta\theta}^2 = & \; u_{\theta_{0M}}U_{\theta_0 M}{}^2\left(\frac{\partial\Delta\theta}{\partial\theta_0}\right)^2 + u_{\theta_{0D}}U_{\theta_0 D}{}^2\left(\frac{\partial\Delta\theta}{\partial\theta_0}\right)^2 + u_{\theta_{1M}}U_{\theta_1 M}{}^2\left(\frac{\partial\Delta\theta}{\partial\theta_1}\right)^2 + u_{\theta_{1D}}U_{\theta_1 D}{}^2\left(\frac{\partial\Delta\theta}{\partial\theta_1}\right)^2 + 2u_{\theta_{0M}}2U_{\theta_0 M}{}^2\frac{\partial\Delta\theta}{\partial\theta_0}\frac{\partial\Delta\theta}{\partial\theta_1} \\ = & \; u_{\theta_{0M}}U_{\theta_0 M}{}^2 + u_{\theta_{0D}}U_{\theta_0 D}{}^2 + u_{\theta_{1M}}U_{\theta_1 M}{}^2 + u_{\theta_{1D}}U_{\theta_1 D}{}^2 - 2u_{\theta_{0M}}u_{\theta_1} \end{aligned} \tag{32}$$

where r is the correlation coefficient. If ~~assume that~~ $\cancel{u_{\theta_{0M}} = u_{\theta_{1M}} = u_{\theta_M}}$ assumed that $U_{\theta_0 M} = U_{\theta_1 M} = U_{\theta_M}$ are fully correlated and $\cancel{u_{\theta_{0D}} = u_{\theta_{1D}} = u_{\theta_D}}$ $U_{\theta_0 D} = U_{\theta_1 D} = U_{\theta_D}$ are uncorrelated we end up with

$$uU^2_{\Delta\theta} = 2u_{\theta_M}2U_{\theta M}{}^2 + 2u_{\theta_D}2U_{\theta D}{}^2 -2u_{\theta_M}-2U_{\theta M}{}^2 = 2u_{\theta_D}2U_{\theta D}{}^2, \tag{33}$$

where $\cancel{u_{\theta_D}}$ $U_{\theta D}$ is the same as $\cancel{u_{\theta_0}}$ U_{θ_0} in Eq. (28).

Now, $\Delta\theta$ is in essence our best estimate of the beam width as expressed through Eq. (17) but the validity of this assumption is associated with some uncertainty. As we shall see in Sect. 5.1 the beam radius estimated with this method does resemble what we would expect from a theoretical calculation of the beam radius, but on the other hand there is no reason to believe it to be a completely correct estimate either. This uncertainty must be incorporated into $\cancel{u_{\Delta\theta}}$ $U_{\Delta\theta}$ and we do this by adding the term $\cancel{u_{\theta_w}}$ ~~such that~~ U_{θ_w} such that

$$uU^2_{\Delta\theta} = 2u_{\theta_D}2U_{\theta D}{}^2 + uU^2_{\theta_w}. \tag{34}$$

As mentioned above $\cancel{u_{\theta_w}}$ U_{θ_w} is quite large and in the following we will assume it to be 100% in relative terms such that $\cancel{u_{\theta_w} = \Delta\theta}$ $U_{\theta_w} = \Delta\theta$. For the smallest beam tested in this study we have $\Delta\theta = 0.01°$ and this leads to an uncertainty originating from $\cancel{u_{\Delta\theta}}$ $U_{\Delta\theta}$ of about 0.069% out of a total of 0.074% and $\cancel{u_{\Delta\theta}}$ $U_{\Delta\theta}$ is thus seen to be the dominant term in $\cancel{u_{b_c}}$ U_{b_c}.

4.3 Overall calibration uncertainty

We can finally find the overall measurement uncertainty. The lidar estimate of the wheel speed is the compensated calibration constant times the reference wheel speed

$$V_{\text{LOS}} = V_{\text{wheel}} \cdot b_c, \tag{35}$$

and the squared uncertainty therefore becomes

$$uU^2_{V_{\text{LOS}}} = uU^2_{V_{\text{wheel}}} b_c^2 + u_{c_c}U_{b_c}{}^2 V^2_{\text{wheel}}, \tag{36}$$

and relative to V_{wheel}

$$\left(\frac{u_{V_{\text{wheel}}}}{V_{\text{LOS}}} \frac{U_{V_{\text{LOS}}}}{V_{\text{wheel}}} \right)^2 = \left(\frac{u_{V_{\text{wheel}}}}{V_{\text{wheel}}} \frac{U_{V_{\text{wheel}}}}{V_{\text{wheel}}} b_c \right)^2 + uU^2_{b_c}. \tag{37}$$

This means that $\cancel{u_{b_c}}$ ~~and therefore~~ $\cancel{u_{\Delta\theta}}$ U_{b_c} and therefore $U_{\Delta\theta}$ is the main contributor to the overall calibration uncertainty.

5 Calibration measurements

In this section will be presented calibration measurements made with different beam widths and for different reference speeds.

5.1 Beam width

It is clear from the uncertainty analysis in Sect. 4 that the beam radius, expressed through $\Delta\theta$, is of great importance for the overall calibration uncertainty. However, how to establish the beam width is not trivial even though our beam is well-behaved and can be well approximated by a pure Gaussian beam and the equations describing this, see ~~Sect.~~Appendix C. For Gaussian beams in general the $1/e$ or $1/e^2$ width of either the electrical field or irradiance is often used to define the beam radius but in our case it must be defined as the width from which it is possible to detect a signal and this depends on several parameters such as the detection threshold, scattering properties of the wheel surface, and also the angle between beam and wheel surface. The best way we have of quantifying this is therefore to measure the tilt angles where we first detect a signal and where we constantly see a signal, respectively. It is clear that there is no guarantee that these angles represent the beam width and it is therefore associated with a significant uncertainty but it is the best estimate we can make with the data at hand.

Following the procedure outlined in Sect. 3.6 we have carried out a series of calibrations with different focus of the beam ranging from about 1 m to 5 m resulting in different beam widths at the wheel. Fig. 8 shows the measured beam radii as function of focus distance calculated from Eq. 17. Shown is also the theoretical $1/e^2$ radii of the irradiance calculated using the standard equations for Gaussian beams. The first thing to notice is ~~that the~~ the clear resemblance in the shape of the two curves ~~resemble each other quite well~~ indicating that this ~~way of estimating the width does actually capture some of the truth about it at least relatively. The~~ is a valid method for estimating the beam width although the absolute values do not agree. Actually, the values of the calculated widths are about three times higher than the measured, but this is not too disturbing since we are not expecting the measured width to represent the $1/e^2$-width but rather the width from where we can detect a signal. More concerning is that the minimum around 1.5 m is not nearly as sharply defined for the measured values as for the theoretical and some of this could possibly be due the finite resolution of the angle measurement but probably not all of it. The minimum beam radius of 0.14 ~~m~~ mm located at 1.53 m and 1.78 m actually corresponds to $\Delta\theta = 0.01°$ which is the same as the angle measurement resolution. Finally, there is the point at 4.03 m which could look like an outlier; the beam width should not be higher with the focus at 4.03 m than at 5.03 m but this has not been clarified. All in all it is very difficult do determine the beam radius and it is thus associated with a large uncertainty. In order to put some numbers on we estimate a relative uncertainty of 30% for the larger beam radii and 50% and even 100% for the smallest beams. The resulting absolute uncertainties can be seen in Table 3 together with the theoretical and measured beam width for each focus distance.

Figures 9 and 10 show two examples of the calibrations made. Figure 9 is made with the laser beam focused at $1.53\ \mathrm{m}$ and thus with the beam waist located very near the top of the wheel so that the beam width on the wheel is about as small as the setup allows while in Fig. 10 the focus is placed at $2.53\ \mathrm{m}$. The mean reference speed is $10.93\ \mathrm{m/s}$. It is clearly seen how $\frac{V_{\mathrm{LOS}}}{V_{\mathrm{wheel}}}$ in general falls off linearly as function of tilt angle as predicted by the models. However, it is also seen that on top of this trend are some discrete steps, something that is also reflected in the residual plot. These steps are due to the narrow beam width resulting in the range of sensed speed being smaller than the resolution of the lidar's Doppler spectrum resulting in the speed estimation to jump from bin to bin quite abruptly. In contrast, this feature is almost completely gone in Figure 10 where the beam is much bigger and therefore a larger range of radial velocities is covered in each measurement ~~widening~~ which spreads

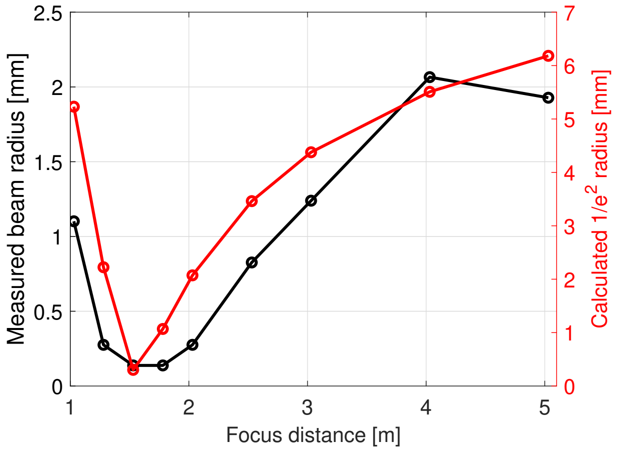

Figure 8. Comparison between the measured beam widths and the theoretically calculated $1/e^2$ radius as function of focus distance.

Table 3. Theoretical and measured beam widths together with estimated uncertainties for the different focus distances used.

Focus distance [m]	Theo. beam radius [mm]	Meas. beam radius [mm]	Beam radius uncertainty [mm]
1.03	5.23	1.10	0.41
1.28	2.22	0.28	0.14
1.53	0.30	0.14	0.14
1.78	1.07	0.14	0.14
2.03	2.07	0.28	0.21
2.53	3.46	0.83	0.28
3.03	4.38	1.24	0.41
4.03	5.51	2.07	0.69
5.03	6.19	1.93	0.69

the Doppler signal over ~~more~~ several bins. This binning effect has an impact on the fit result through the standard error on the slope and intercept which is indeed higher for the narrow beam, but as mentioned in Sect. 4.2 this effect is still much smaller than other uncertainty contributions. This smoothing effect of the regression can also be seen in the residual plots (lower panel) which have average values of essentially 0 (ranges between $2.3 \cdot 10^{-14}$ and $-2.1 \cdot 10^{-14}$ for Fig. 9 and Fig. 10, respectively) meaning the fit is very close to the average. The red line in the top panel of the figures is the least-squares fit of a straight line to the measurement data over the range of tilt angles indicated by the extend of the red line itself. The fit ranges over angles from $\theta_0 + 0.1°$ to $0.1°$ before the maximum measured tilt angle. The resulting fit parameters, slope and intercept, are shown in the insets.

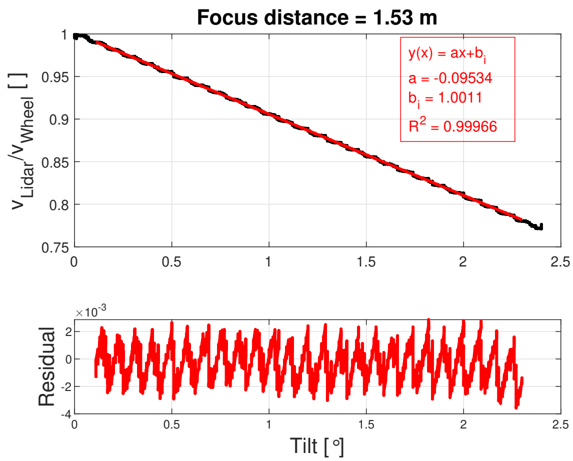

Figure 9. Example of calibration measurement made with a focus setting of 1.53 m meaning that the waist of the beam is placed very near the top of the wheel. The black curve is the measurement data and the red a least-squares fit of a straight line to the data. In the lower panels is shown the residuals of the fit.

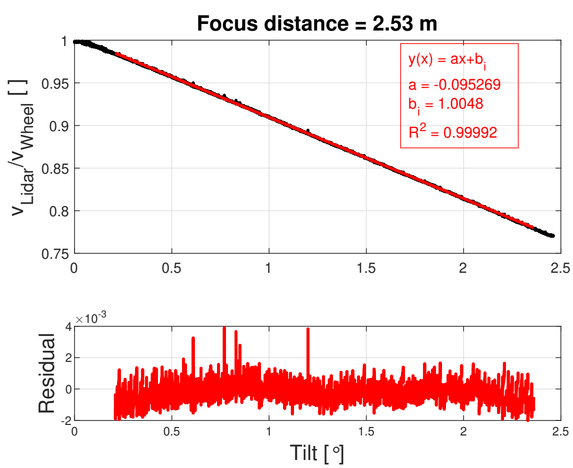

Figure 10. Example of calibration measurement made with a focus setting of 2.53 m. The black curve is the measurement data and the red a least-squares fit of a straight line to the data. In the lower panels is shown the residuals of the fit.

Figure 11 shows the fit slopes and intercepts for all nine calibrations as function of focus distance. According to the narrow beam model the slope of $\frac{V_{\mathrm{LOS}}}{V_{\mathrm{wheel}}}$ is $-\frac{L}{R}$ which with the parameters specified in Table ~~?? equals −9.60 %~~ 1 equals −9.60 percent per degree and from the figures it is seen that the measured slopes range from ~~−9.496 %/∘ to −9.537 %/∘~~ −9.496 to −9.537 percent per degree. This is not a large difference but it is still larger than the estimated uncertainty and it is more or less the same for all calibrations and not just one or two outliers. The reason behind this deviation is not known.

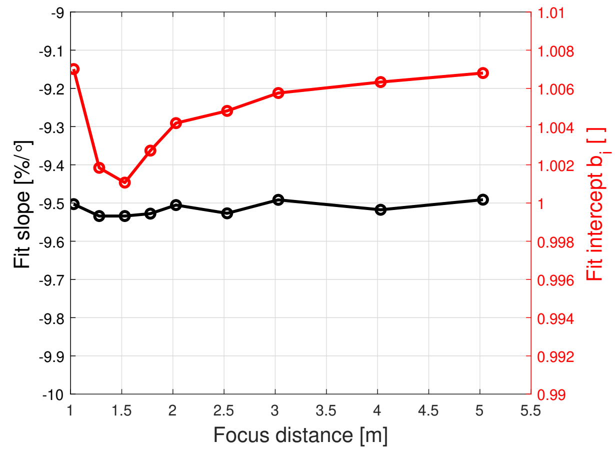

Figure 11. Fit slope and intercept as function of focus distance. The intercept values show a clear minimum at $1.53\ \mathrm{m}$ where the beam with at the wheel is smallest clearly illustrating the need for compensating these results.

More interesting for the calibration purpose is of course the fit intercept which is shown in red in Fig. 11. It is clearly seen that the intercept overestimates as expected and in shape the curve looks a lot like the measured beam width in Fig. 8. This highlights the need to compensate the calibration result for this. This has been done in Fig.12 where the red curve shows the compensated intercept values and the black curves represent the estimated standard uncertainties. The compensation has clearly brought the intercept closer to 1 with the maximum and minimum placed approximately 0.3% on either side. Most of the points are within or very close to the estimated standard uncertainty with the exception of the points at $1.78\ \mathrm{m}$ and $2.03\ \mathrm{m}$. This is probably due to the measurement of $\Delta\theta$ which seems low compared to the theoretical value as seen in Fig. 8 and therefore the compensation becomes too weak. The combined uncertainties calculated using the equations derived in ~~Sec.~~Sect. 4 range from about 0.08% for the narrow beams up to about 0.9% for the widest beams, and it is clearly seen how the shape of the uncertainty curve follows that of the measured beam width in Fig. 8. This is due to the term $\cancel{u_{\theta_w}}$ U_{θ_w} which we have estimated to be equal to the value of $\Delta\theta$ and which is dominating. This underlines the importance of a good estimate of the beam width.

5.2 Different reference speeds

In this section we present the results of calibrations made with different reference speeds but a fixed focus distance of $1.53\ \mathrm{m}$, i.e. with the smallest possible beam width at the wheel.

The tested reference speeds range from about 3.3 $\mathrm{m/s}$ to 17.3 $\mathrm{m/s}$, and Figs. 13 and 14 show two examples of measurements and fits made at $5.44\ \mathrm{m/s}$ and $13.89\ \mathrm{m/s}$, respectively. In both cases there is a very good agreement with what is expected from the model as well as with the results in Sect. 5.1. It is noted that the characteristic staircase shape also seen in Fig. 9 is very pronounced in both these figures, but that the length of each "step" seems to change with the reference wheel speed. This

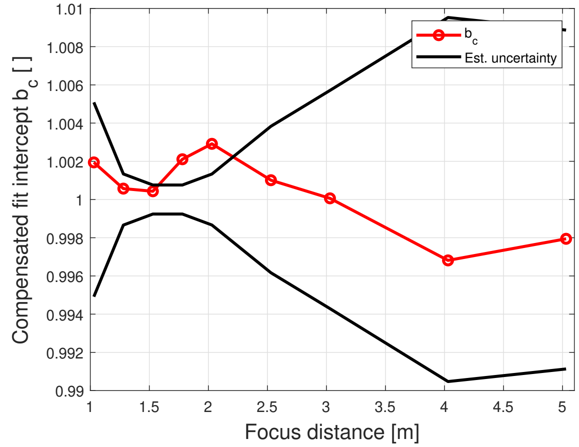

Figure 12. Compensated regression intercepts together with the estimated standard uncertainties.

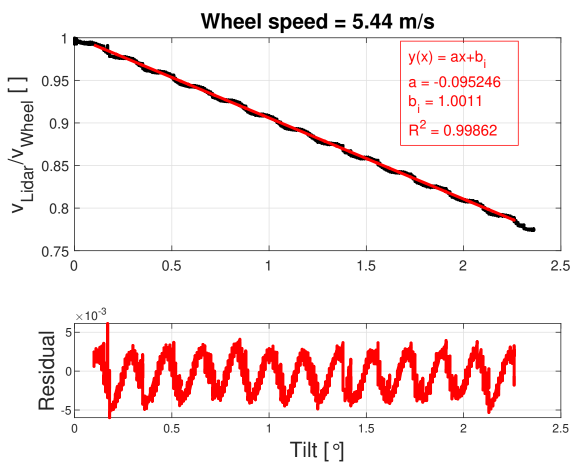

Figure 13. Example of calibration measurement made with a reference speed $5.44\ \mathrm{m/s}$ and a focus distance of $1.53\ \mathrm{m}$. The black curve is the measurement data and the red a least-squares fit of a straight line to the data. In the lower panels is shown the residuals of the fit showing some distinct oscillations because of the speed estimation jumping from bin to bin due to the very narrow beam.

is because that what is plotted is the ratio between measured and reference speed and for low reference speeds the bins of the Doppler spectra becomes relatively larger as function of tilt angle.

Fig. 15 shows the resulting fit parameters for all the tested reference speeds. We see that the slope of the fit lies between ~~$-9.51\%/°$ $-9.56\%/°$ and~~ -9.51 and -9.56 percent per degree and is more or less constant across the tested speeds. Also the fit intercept is very close to constant for the first five tested speeds and is bounded within 0.998 and 1.002, and thus within the estimated uncertainty, but the last point at 17.26 m/s stands out a bit. Here the intercept drops to below 1, but is still

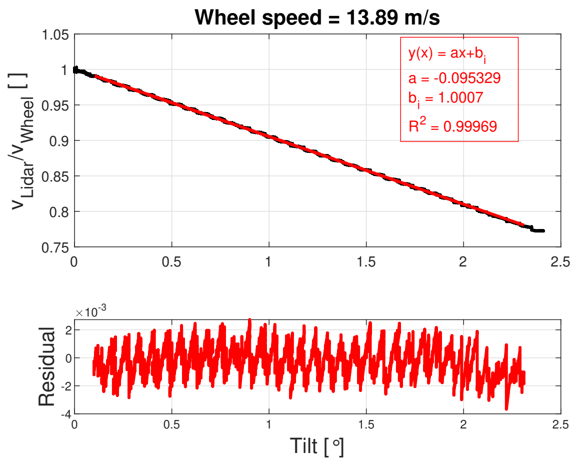

Figure 14. Example of calibration measurement made with a reference speed $13.89\ \mathrm{m/s}$ and a focus distance of $1.53\ \mathrm{m}$.

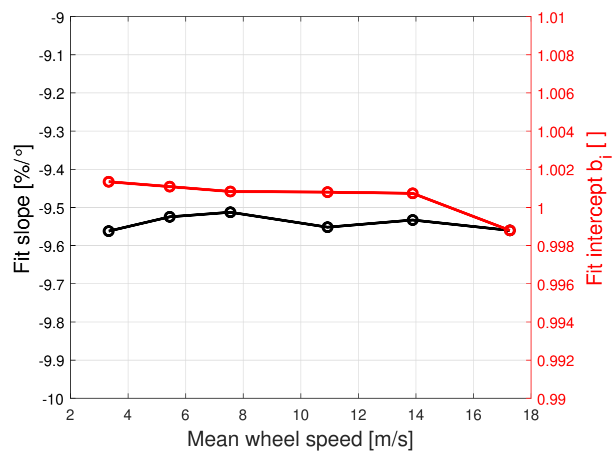

Figure 15. Results of fits for different reference speeds. Fit intercept not compensated for w.

within the uncertainty. A possible explanation for this is that at 17 m/s the wheel rotates at around 9.5 revolutions per second which is quite fast and the entire rig including transceiver and inclinometer starts to shake which limits both lidar and angle measurement.

Again the regression intercepts have been compensated and the result is shown in Fig. 16 together with the uncertainties. Because of the small beam width used in these measurements the difference between b_i and b_c is very small. The assumed uncertainty on $\Delta\theta$ is the same as for the same focus distance in the previous section and the resulting combined standard uncertainty is about 0.08% which most of the points lie close to.

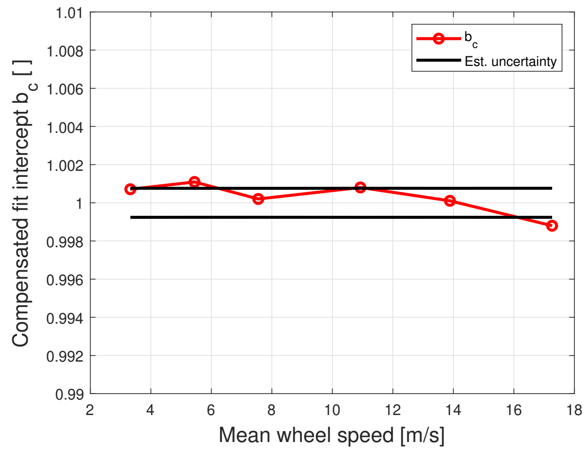

Figure 16. Compensated fit intercepts together with the estimated standard uncertainties.

6 Discussion

It can seem paradoxical to use a flywheel to calibrate a Doppler wind lidar when the parameter we want to measure, the peripheral speed, is the one thing the lidar can not measure. ~~Instead~~ Nevertheless, the presented measurements and analysis show that the proposed calibration method is not only practically feasible but could actually lead to a significant reduction in calibration uncertainty compared to the current practice. However, there could also be other methods for achieving a similar calibration result. For instance, it seems more straight forward to measure a linear motion along the direction of the beam and this might very well be the case ~~. For example,~~ because besides directly measuring the desired parameter, the uncertainties introduced by the angle measurement and assessing the zero-point of the angle scale together with the beam width can be alleviated. ~~However~~On the other hand, there are also arguments for using the flywheel; as discussed earlier by scanning a range of speeds and fitting the inherent uncertainty due to discretisation is reduced, and the symmetrical nature of the wheel makes it easy to obtain a very stable reference speed whereas with a linear motion the target would probably have to be moved back and forth and thus accelerated up to a known speed repeatedly. This would then require the position of the reference target to logged together with it's speed which again demands a more complicated geometrical model. Another idea could be to measure in a range of angles covering the direction toward the centre of the wheel. In this way, a zero-point defined as the angle where the beam is perpendicular to the wheel surface could be established as where no speed is measured thus alleviating the problems seen above with finding θ_0 ~~,~~ and possibly θ_1~~, seen above.~~. In this case the calibration uncertainty would depend critically on the angle measurement uncertainty. Unfortunately, the calibration setup ~~in it's present state~~ does not allow for such a measurement to be made due to limitations in the attainable tilt angles.

The uncertainty analysis shows that the main uncertainty contributor is $U_{\Delta\theta}$ which essentially depends on the beam width estimation. An estimate for $\Delta\theta$ based on the tilt angles for the first sporadic and the first stable measurements, respectively, was proposed. Another approach that could potentially reduce this uncertainty is to measure the backscatter level as function of tilt angle. In this way the backscatter signal would increase strongly from θ_0 to θ_1 as the overlap between beam and wheel increases and then remain more or less constant when the entire beam is on the beam. Unfortunately, our lidar in its present state does not measure or store the backscatter level and therefore this approach has not been tested.

7 Conclusions

Inspired by a similar concept commonly used for calibrating LDAs we have constructed a setup for calibrating coherent Doppler wind lidars based on a spinning flywheel with the lidar beam skimming the wheel periphery. The setup is made in such a way that the laser beam can be tilted and thus probing different projections of the wheel's tangential speed. A simple model shows that there is a linear relation between the beam tilt angle and the measured LOS speed and this can be utilised to extrapolate back to the true tangential speed at zero tilt; the one angle otherwise impossible to measure at because the physical overlap between wheel surface and laser beam disappears. The model takes into account the finite width of the laser beam but only under the assumption that the beam is collimated while in reality the beam used in the tests is actually focused in order to control the beam radius. The model also forms the basis of the uncertainty analysis which concludes that a total calibration standard uncertainty of about 0.1% can be achieved with this setup which is approximately an order of magnitude better than current practice. The uncertainty analysis reveals that the main contributor to the total uncertainty is the finite radius of the laser beam and in order to reduce the uncertainty it is essential to determine this better than we have been able to achieve so far. Calibration measurements performed at different reference speeds and with different beam widths all show a good agreement with the model and confirms that the lowest calibration uncertainty is achieved when the beam width is minimised.

Code and data availability. The measurements and scripts for data analysis is available via (Pedersen, 2020).

Appendix A: Approximation to 1D model

In this section how the ratio $\frac{V_{\text{LOS}}}{V_{\text{wheel}}}$ as function of tilt angle for a beam of small but finite width is approximately the same as that for an infinitely narrow beam.

If we apply Taylor's expansion to the third order to Eq. (8) we get

$$\begin{aligned}
\frac{V_{\text{LOS}}}{V_{\text{wheel}}} &\approx \frac{1}{\Delta\phi_r}\left(\phi_{r_1} - \frac{1}{6}\phi_{r_1}^3 - \phi_{r_0} + \frac{1}{6}\phi_{r_0}^3\right) \\
&\approx \frac{1}{\Delta\phi_r}\left(\Delta\phi_r - \frac{1}{6}\left(\phi_{r_1}^3 - \phi_{r_0}^3\right)\right) \\
&\approx 1 - \frac{1}{6}(\phi_{r_1}^2 + \phi_{r_0}^2 + \phi_{r_1}\phi_{r_0}),
\end{aligned} \tag{A1}$$

and if we further make the approximations

$$\phi_0 = \phi_{\mathrm{m}} - \delta, \tag{A2}$$

$$\phi_1 = \phi_{\mathrm{m}} + \delta, \tag{A3}$$

where $\phi_{r_{\mathrm{m}}}$ is the mean of ϕ_{r0} and ϕ_{r_1} and δ is a small perturbation we get

$$\frac{V_{\mathrm{LOS}}}{V_{\mathrm{wheel}}} = 1 - \frac{1}{6}(\phi_{r_1}^2 + \phi_{r_0}^2 + \phi_{r_1}\phi_{r_0}) = 1 - \frac{1}{6}\left(3\phi_{\mathrm{m}}^2 + \delta^2\right) \approx 1 - \frac{1}{2}\phi_{\mathrm{m}}^2 \approx \cos\phi_{r_{\mathrm{m}}}, \tag{A4}$$

which is seen to be equal to Eq. (6).

Appendix B: 3D beam

The result of Eq. (15) can be reached in the following way

$$\begin{aligned}
\frac{V_{\mathrm{LOS}}}{V_{\mathrm{Ref}}} &= \frac{\iint\limits_{\mathcal{S}} I(y,z)\cos\phi_r \,\mathrm{d}S}{Ar(\mathcal{S})} \\
&= \frac{\iint I(y,z)\cos\phi_r \sqrt{1+\left(\frac{\partial X(y)}{\partial y}\right)^2+\left(\frac{\partial X(y)}{\partial z}\right)^2}\,\mathrm{d}y\mathrm{d}z}{\iint \sqrt{1+\left(\frac{\partial X(y)}{\partial y}\right)^2+\left(\frac{\partial X(y)}{\partial z}\right)^2}\,\mathrm{d}y\mathrm{d}z} \\
&= \frac{\iint I(y,z)\frac{y-y_r}{R} \sqrt{1+\left(\frac{\partial X(y)}{\partial y}\right)^2+\left(\frac{\partial X(y)}{\partial z}\right)^2}\,\mathrm{d}y\mathrm{d}z}{\iint \sqrt{1+\left(\frac{\partial X(y)}{\partial y}\right)^2+\left(\frac{\partial X(y)}{\partial z}\right)^2}\,\mathrm{d}y\mathrm{d}z} \\
&= \frac{\iint I(y,z)\frac{y-y_r}{R} \sqrt{1+\left(\frac{y-y_r}{\sqrt{R^2-(y-y_r)^2}}\right)^2}\,\mathrm{d}y\mathrm{d}z}{\iint \sqrt{1+\left(\frac{y-y_r}{\sqrt{R^2-(y-y_r)^2}}\right)^2}\,\mathrm{d}y\mathrm{d}z} \\
&= \frac{\iint I(y,z)\frac{y-y_r}{R} \sqrt{\frac{R^2-(y-y_r)^2}{R^2-(y-y_r)^2}+\frac{(y-y_r)^2}{R^2-(y-y_r)^2}}\,\mathrm{d}y\mathrm{d}z}{\iint I(y,z)\sqrt{\frac{R^2-(y-y_r)^2}{R^2-(y-y_r)^2}+\frac{(y-y_r)^2}{R^2-(y-y_r)^2}}\,\mathrm{d}y\mathrm{d}z} \\
&= \frac{\iint I(y,z)\frac{y-y_r}{R} \sqrt{\frac{R^2}{R^2-(y-y_r)^2}}\,\mathrm{d}y\mathrm{d}z}{\iint I(y,z)\sqrt{\frac{R^2}{R^2-(y-y_r)^2}}\,\mathrm{d}y\mathrm{d}z} \\
&= \frac{\iint I(y,z)\frac{y-y_r}{\sqrt{R^2-(y-y_r)^2}}\,\mathrm{d}y\mathrm{d}z}{\iint \frac{R}{\sqrt{R^2-(y-y_r)^2}}\,\mathrm{d}y\mathrm{d}z}.
\end{aligned} \tag{B1}$$

Appendix C: Width of Gaussian beam

The theoretical beam width at the top of the wheel can calculated by appropriate combination of the following two equations: The width of an untruncated Gaussian beam at a distance x' from the beam waist can be calculated through

$$w(x') = w_0 \sqrt{1 + \left(\frac{\lambda x'}{\pi w_0^2}\right)^2}, \tag{C1}$$

where w_0 is the width at the waist and λ is the laser wavelength, ~~Siegman (1986)~~(Siegman, 1986). Similarly can w_0 with the waist placed a distance x from the focusing lens be found as

$$w_0(x) = \sqrt{\frac{w_l^2 - \sqrt{w_l^4 - 4\left(\frac{\lambda x}{\pi}\right)^2}}{2}}, \tag{C2}$$

where w_l is the beam width at the lens.

Author contributions. Anders Tegtmeier Pedersen: Measurements, data processing, data analysis, model development, manuscript writing. Michael Courtney: Conceptual idea, model development, manuscript writing.

Competing interests. The authors declare that they have no conflict of interest.

Disclaimer. TEXT

Acknowledgements. This work has been performed under the Danish EUDP project *TrueWind*, journal number 64015-0635. Professor Torben Mikkelsen and Steen Andreasen are gratefully acknowledged for initiating, designing, and constructing the calibration rig. All members of the DTU Wind Energy, TEM, Measurement Systems Engineering team are thanked for their great help and support. The anonymous reviewers are gratefully thanked for thorough and constructive criticism.

References

AMO GmbH: Incremental angle measuring systems based on the AMOSIN – Inductive Measuring Principle, http://www.amoitalia.it/pdf/Catalogo%20rotativi_WMI_EN_2013_08_21.pdf(accessedFebruary21,2020), 2013.

Angelou, N., Foroughi Abari, F., Mann, J., Mikkelsen, T., and Sjöholm, M.: Challenges in noise removal from Doppler spectra acquired by a continuous-wave lidar, in: Proceedings of the 26th International Laser Radar Conference, 2012.

Bean, V. and Hall, J.: New primary standards for air speed measurement at NIST, Metrology - at the Threshold of the Century Are We Ready?, pp. 413–421, 1999.

Courtney, M.: Calibrating nacelle lidars, DTU Wind Energy E-0020, 2013.

Cverna, F.: ASM ready reference - Thermal properties of metals, ASM International, 2002.

Duncan, M. L. and Keck, J.: Considerations for Calibrating a Laser Doppler Anemometer, in: Proceedings of Measurement Science Conference (MSC), 2009.

Joint Committee for Guides in Metrology: Evaluation of measurement data — Guide to the expression of uncertainty in measurement, https://www.bipm.org/utils/common/documents/jcgm/JCGM_100_2008_E.pdf, 2008.

Joint Committee for Guides in Metrology: International vocabulary of metrology – Basic and general concepts and associated terms (VIM), https://www.bipm.org/utils/common/documents/jcgm/JCGM_200_2012.pdf, 2012.

Lee, A. J. and Seber, G. A. F.: Linear regression analysis, Wiley, 2003.

Pearson, G. N., Roberts, P. J., Eacock, J. R., and Harris, M.: Analysis of the performance of a coherent pulsed fiber lidar for aerosol backscatter applications, Applied Optics, 41, 6442–6450, 2002.

Pedersen, A., Foroughi Abari, F., Mann, J., and Mikkelsen, T.: Theoretical and experimental signal-to-noise ratio assessment in new direction sensing continuous-wave Doppler lidar, in: Journal of Physics: Conference Series (Online), vol. 524, IOP Publishing, https://doi.org/10.1088/1742-6596/524/1/012004, content from this work may be used under the terms of the Creative Commons Attribution 3.0 licence. Any further distribution of this work must maintain attribution to the author(s) and the title of the work, journal citation and DOI. Published under licence by IOP Publishing Ltd, 2014.

Pedersen, A. T.: Flywheel calibration of coherent Doppler wind lidar - data, https://doi.org/10.11583/DTU.11991189, 2020.

Shinder, I. I., Crowley, C. J., Filla, B. J., Moldover, M. R., Stop, M., and Drive, B.: Presented at the 16 th International Flow Measurement Conference , Flomeko 2013 IMPROVEMENTS TO NIST ' S AIR SPEED CALIBRATION SERVICE Realizing the primary standard, in: International Flow Measurement Conference, pp. 1–9, 2013.

Siegman, A. E.: Lasers, University Science Books, https://app.knovel.com/hotlink/toc/id:kpL000001E/lasers/lasers, 1986.

Wagenaar, J., Bedon, G., Werkhoven, E., and van Diggelen, C.: Wind Iris nacelle LiDAR calibration at ECN test site, ECN-X–16-116, 2016.